Journal of Molecular Catalysis A: Chemical 392 (2014) 31–38

Contents lists available at ScienceDirect

Journal of Molecular Catalysis A: Chemical

journal homepage: www.elsevier.com/locate/molcata

Synthesis and characterization of phosphate anchored MnO_2 catalyzed solvent free synthesis of xanthene laser dyes

G. Harichandran [a,*], S. David Amalraj [a], P. Shanmugam [b,*]

[a] Department of Polymer Science, University of Madras, Guindy Campus, Chennai 600 025, India
[b] Organic Chemistry Division, CSIR-Central Leather Research Institute, Adyar, Chennai 600 020, India

ARTICLE INFO

Article history:
Received 1 August 2013
Received in revised form 22 April 2014
Accepted 27 April 2014
Available online 10 May 2014

Keywords:
P-MnO_2 catalyst
1,8-Dioxooctahydroxanthene
14-Aryl(alkyl)-14H-dibenzo[a,j]xanthene
Laser dye
Solvent-free synthesis

ABSTRACT

A highly stable and environmentally benign phosphate anchored MnO_2 (*P*-MnO_2) catalyst has been prepared. The catalyst has been characterized by using TGA, FTIR, Raman, XRD, UV-DRS, XPS, FESEM, and EDAX techniques. The catalytic behavior of *P*-MnO_2 has been demonstrated for the synthesis of 1,8-dioxooctahydroxanthene and 14-aryl (alkyl)-14H-dibenzo[a,j]xanthene laser dye derivatives under solvent free conditions. Recyclability, high yield, short reaction time, relative non-toxicity and easy workup are the advantages of the presented catalyst.

1. Introduction

The development of newer synthetic methods based on green chemistry processes is increasingly of interest in organic synthesis due to economic and environmental concerns. Owing to the growing environmental concern, advancement of green processes using heterogeneous catalysts under solvent free conditions has awakened great interest in recent years. Solvent free heterogeneous catalysis makes organic synthesis simpler, saves energy, and prevents wastage of solvent, chemical hazards and toxicity [1]. Since heterogeneous catalysts play a key role in organic transformations a number of catalysts have been developed. Solid acid catalysts have advantage over homogeneous acid catalysts as they can be easily recovered from reaction mixture by filtration and can be reused several times, without loss of active sites, thereby making the process more economically and environmentally viable. Heterogeneous catalysts anchored or impregnated with phosphoric acid over the metal oxide phases have been widely used in industry for decades, e.g. in olefin hydration to alcohols, propylene oligomerisation, alkylation and isomerization of 1-butene [2–4]. Thus, there are efforts to develop new solid acid catalysts and to demonstrate their catalytic application in organic transformations [5].

In the current investigation, a phosphate anchored manganese oxide ($Mn(H_2PO_4)_2{\cdot}2H_2O$) with enhanced catalytic property, increased surface acidity, stabilized surface area and crystal phase has been prepared [6]. Xanthenes and benzoxanthenes are important classes of heterocyclic compounds used as leuco dyes in laser technology [7] and pH sensitive fluorescent materials for the visualization of biomolecules [8]. Moreover, these compounds have received great attention due to their therapeutic and biological properties such as antibacterial [9], antiviral [10] and anti-inflammatory [11] properties; and their use in photodynamic therapy [12] and in antagonism of the paralyzing action of zoxazolamine [13]. Several methods have been reported for the syntheses of 1,8-dioxooctahydroxanthene and 14-aryl-14*H*-dibenzo[a,j]xanthene using a number of catalysts [14–37]. However, application of the new catalyst $Mn(H_2PO_4)_2{\cdot}2H_2O$ (*P*-MnO_2) in the synthesis of these compounds has not been reported so far. We demonstrate the efficacy of this catalyst in the synthesis of xanthene derivatives via a multicomponent reaction under solvent-free condition.

2. Experimental

2.1. Characterization

Melting points were determined in open capillaries and are uncorrected. Chromatography purification was conducted by column chromatography using silica gel. Solvents used for purification

* Corresponding authors. Tel.: +91 44 22202821.
E-mail addresses: umghari@gmail.com, umhari@yahoo.co.in (G. Harichandran).

http://dx.doi.org/10.1016/j.molcata.2014.04.035
1381-1169/

were of commercial grade and were purified before use. FT-IR spectra were recorded on a Thermo Mattson Satellite – 3000 spectrophotometer by Nujol mull and KBr pellet methods. ^{1}H and ^{13}C NMR spectra were recorded on a Bruker ultra shield spectrometer (300 and 75 MHz) or a JEOL-500 MHz spectrometer (500 and 125 MHz) in $CDCl_3$ solvent using TMS as internal standard. Mass spectra were recorded on JEOL GCMATE II GC-MS Mass spectrometer. The TG experiments were carried out in air on a NETZSCH STA 490C-CD apparatus by increasing the temperature at a rate of 10 °C/min from 50 to 800 °C with calcined Al_2O_3 powder as the standard reference. FE-SEM/EDAX analyses were carried out on a HITACHIS-3400N microscope. The phase composition and crystalline nature of the catalyst were analyzed using PXRD. Bruker D8 ADVANCE MODEL diffractometer was used for recording PXRD data between 2θ values ranging from 20° to 70° using Cu Kα as source operating at 40 kV and 30 mA. XPS measurements were performed with Omicron Nanotechnology, GmBH, Germany, XM1000-monochromator with Al Kα radiation of 1483 eV operated at 300 W (20 mA emission current, 15 kV) and a base pressure of 5×10^{-5} mbar. The survey scan was performed with a step size of 0.5 eV along with 50 eV as the pass energy. The high-resolution scan was done with 0.03 eV as the step size and 20 eV as the pass energy with three sweep segments. Raman spectra were recorded using a BRUKER RFS 27: Stand-alone FT-Raman Spectrometer equipped with Nd:YAG 1064 nm as the excitation source.

2.2. Spectroscopic data for selected compounds

2.2.1. 9-(2-Thienyl)-3,3,6,6-tetramethyl-1,2,3,4,5,6,7,8-octahydroxanthene-1,8-dione **5h**

White solid, m.p. 145 °C; FT-IR (KBr) ν_{max}: 2900, 1643, 1373, 1249, 995, 648 cm^{-1}; ^{1}H NMR (500 MHz, $CDCl_3$) δ_H: 7.03–7.02 (m, 1H, ArH), 6.97–6.96 (m, 1H), 6.84–6.82 (m, 1H), 5.15 (s, 1H, CH), 2.46 (s, 4H, $(CH_2)_2$), 2.26 (s, 4H, $(CH_2)_2$), 1.11 (s, 6H, $(CH_3)_2$), 1.06 (s, 6H, $(CH_3)_2$); ^{13}C NMR (125 MHz, $CDCl_3$) δ_C: 196.4, 162.8, 148.2, 126.9, 125.4, 123.5, 115.3, 50.8, 40.9, 32.3, 29.4, 27.4, 26.4.

2.2.2. 9-(2-Ferrocenyl)-3,3,6,6-tetramethyl-1,2,3,4,5,6,7,8-octahydroxanthene-1,8-dione **5i**

Brown solid, m.p. 220 °C; FTIR (KBr) ν_{max}: 2962, 2869, 1658, 1365, 1195, 1134, 026, 802, 671, 570 cm^{-1}; ^{1}H NMR (500 MHz, $CDCl_3$) δ_H: 4.65 (s, 1H, CH), 4.08–3.99 (m, 7H), 3.82 (s, 2H), 2.45–2.32 (m, 8H, $(CH_2)_4$), 1.16 (s, 6H, $(CH_3)_2$), 1.14 (s, 6H, $(CH_3)_2$); ^{13}C NMR (125 MHz, $CDCl_3$) δ_C: 196.8, 164.1, 116.3, 68.9, 67.0, 66.5, 51.0, 41.1, 32.0, 29.8, 27.2, 23.5. Mass (ESI) calcd. for $C_{27}H_{30}FeO_3$: 458.3703; found: 458.4198.

3. Results and discussion

3.1. Thermal analysis

The TG curve for MnO_2 showed weight loss in the range of 100–310 °C, and was about 4.1 wt %, which is attributed to the loss of the adsorbed water molecules. The TG curves of *P*-MnO_2 are shown in Fig. 1. The TG curve shows the mass losses between 30 and 800 °C, which are related to the elimination of water molecules and the phase transformations. The elimination of water was observed at three ranges: 25–120, 120–197 and 197–293 °C. The corresponding observed mass losses are 19.88%, 5.71% and 6.69%, respectively. The thermal decomposition of $Mn(H_2PO_4)_2{\cdot}2H_2O$ involves the dehydration of the co-ordinated water molecules and the intramolecular dehydration of the protonated phosphate groups. There is a gradual mass loss (about 7.31%) in the range of 293–800 °C. This is possibly related to the reaction between $Mn_2P_4O_{12}$ and air to form manganese pyrophosphate, $Mn_2P_2O_7$

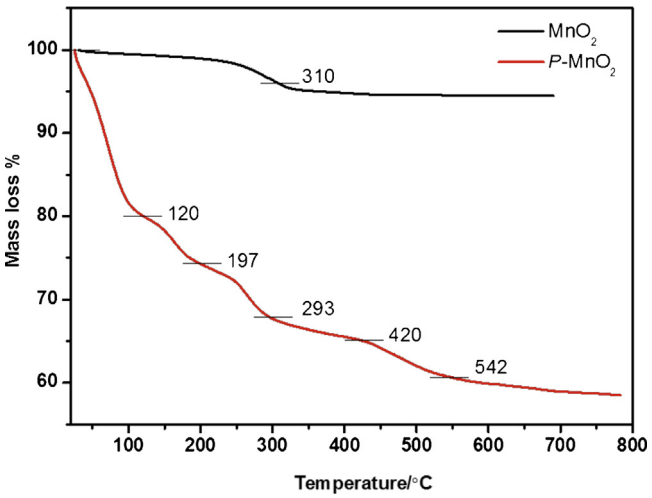

Fig. 1. TGA curves of the synthesized: (a) MnO_2 and (b) *P*-MnO_2.

as indicated in Eq. (1) [38]. The overall reaction could be presented as follows:

$$Mn(H_2PO_4)_2{\cdot}2H_2O \rightarrow Mn_2P_2O_7 + P_2O_5 + 4H_2O \quad (1)$$

3.2. FTIR analysis

The FT-IR spectra of MnO_2 and *P*-MnO_2 are shown in Fig. 2. The FT-IR spectrum of the *P*-MnO_2 catalyst shows bands at 3394 and 1641 cm^{-1}, corresponding to the OH stretching and bending vibrations, respectively. Two bands (3394 and 3217 cm^{-1}) that appear in the region of the hydroxyl stretching are assigned to the strongly H-bonded O–H species and the residual surface hydroxyl groups and ligated H_2O in the catalyst surface. The absorption band at 3217 cm^{-1} is attributed to PO–H stretching (hydrogen phosphates). The absorption bands at 1149 and 1049 cm^{-1} are assigned to antisymmetric and symmetric stretching mode vibrations of the isolated PO_4^{3-} tetrahedra. The absorption bands at 802, 648 and 516 cm^{-1} are assigned to the ν(P–OH) stretching, δ(P–O–Mn) bending and $\nu_4(PO_4^{3-})$, respectively [39,40].

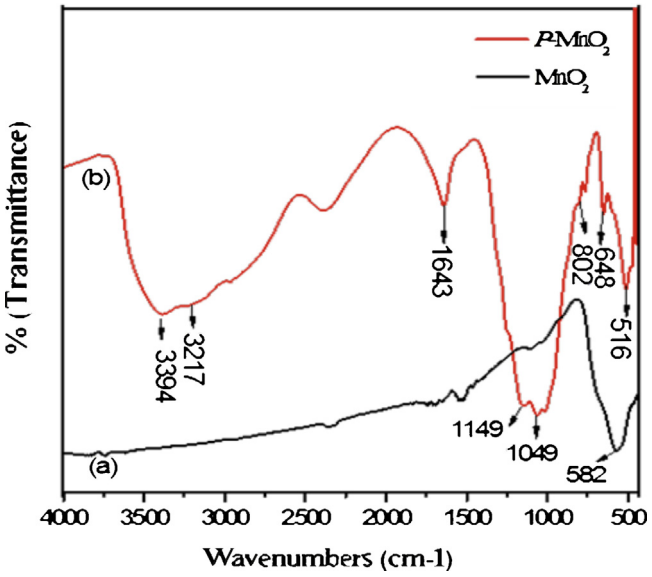

Fig. 2. FT-IR spectra of (a) MnO_2 and (b) *P*-MnO_2 catalyst.